AN ANCIENT INVERTED VALLEY NETWORK PRESERVED BY OLIVINE-RICH VOLCANIC INFILL.

H. F. Zigo[1] and C. S. Edwards[1], M. R. Salvatore[1], [1]Department of Physics and Astronomy, Northern Arizona University, 527 South Beaver Street, Flagstaff, AZ 86001; hfz3@nau.edu

Introduction: Olivine is an abundant mineral in the Solar System, with its presence being observed on objects like Earth, the Moon [e.g. 1], Mars [e.g. 2], and asteroids [e.g. 3]. A notable feature of olivine is its susceptibility to chemical alteration under most aqueous conditions [4]. The presence of olivine still on the surface of Mars indicates an extensive period of dry processes [4]. The distribution and identification of olivine on Mars is complicated by a variety of geologic processes including latitude-dependent mantling [5], making these observations most common towards the equator and more scarce near the poles [6][7]. Of importance for mars, olivine appears to be detected in early Noachian, Hesperian and Amazonian terrains, entailing that there has not been enough fluid movement to weather the olivine so that it is no longer visible from orbit [7]. To better understand the distribution and location of olivine, we began to create a global map of olivine exposures using the highest resolution data to date (100m/pixel). As a part of the construction of this global map, we found evidence for a new and unique type of deposit: olivine-bearing material with a sinuous and branching appearance. This feature is located at 347.582E, -24.967N, southwest of Novara Crater. The goal of this effort is to determine the origin, structure, processes, and timeline of this unique mineralogical and morphological feature.

Methods: Using thermal infrared data from the 2001 Mars Odyssey Thermal Emission Imaging System (THEMIS), we use a red-green-blue decorrelation stretch (DCS) on a 10-band daytime thermal infrared images using bands 8 (11.79 μm), 7 (11.04 μm), and 5 (9.35 μm). In this DCS band combination, olivine appears as a bright purple/magenta color on the surface due to its relatively low emissivity near 11 μm, making it easily identifiable in these products [8]. Using the Java Mission-planning and Analysis for Remote Sensing program (JMARS), we began creating a global map of olivine exposures at a 256 pixels per degree using a new DCS THEMIS mosaic [9]. THEMIS images were processed following the methods described [10], where drift and wobble were removed to correct for focal plane temperature variations, "plaid" was removed to correct for line and column-detector readout noise, and "salt and pepper" white noise was also removed to enhance our ability to identify small-scale compositional features [11]. Following the standard THEMIS image correction routines, images were mosaicked using the methods outlined in [10] where a local or "running" decorrelation stretch is used to help maximize the expression of spectrally differentiable surface units.

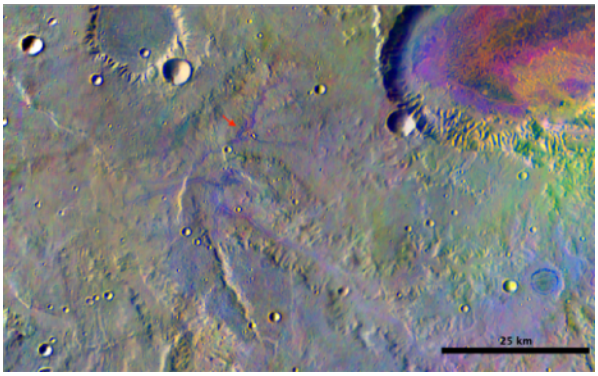

Figure 1. THEMIS DCS 8-7-5 of valley network with olivine bearing material. Image centered at 347.582E, -24.967N which depicts the purple signature of olivine (red arrow) following a sinuous and dendritic pattern.

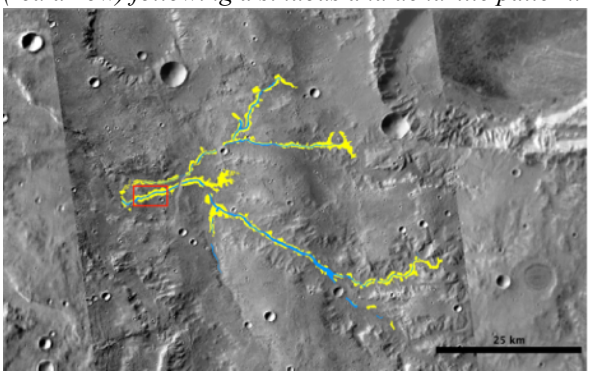

Figure 2. MRO CTX with mapped outline of the proposed valley network. Red box indicates location of Figure 3. The blue outlines the smooth, featureless central portion. The yellow indicates the olivine-rich, rubbly material surrounding the central portion.

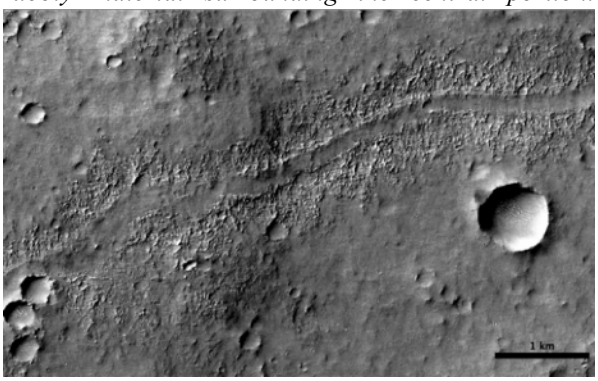

Figure 3. MRO CTX image of a pixel/degree of 8192.

The distinct morphological properties can be observed at this scale. The rough, rubbly terrain is olivine-rich, while the smooth central feature is olivine-poor.
decorrelation stretch is used to help maximize the expression of spectrally differentiable surface units.

Results: The observed pattern of olivine exposures in this location is branching and dendritic in nature with unique morphological, spectral, and thermophysical properties. The distinctive purple signature of olivine present in the branching network is concentrated towards the geographic center of this feature and fades towards both the east and west away from this central location. (Figure 1). While the central feature is discontinuous and only the portion we mapped contains observable olivine exposures surrounding the central feature (as this is the diagnostic criteria for mapping), it is likely that this feature may be more extensive and continuous than its spectral signatures indicate.

Within this geologic unit are two distinct morphologies and compositional properties: an olivine-free central feature with lower thermal inertia and an olivine rich rubble pile on/surrounding the central feature on either side that is topographically higher and exhibits higher thermal inertia. The central portion of the feature is characterized by lower thermal inertia, and an olivine-poor and relatively smooth, featureless, slight topographic depression. The terrain surrounding the main feature is topographically higher, has higher thermal inertia than the surrounding terrain and the central feature, and shows spectral evidence of olivine enrichment in THEMIS data. In order to assist with differentiating units, we used mapping techniques to identify the features not only by their olivine abundance but by their morphology, thermal inertia, and composition. We mapped the main channel (outlined in blue, see Figure 2) and surrounding rubble pile (outlined in yellow, Figure 2) using projected Mars Reconnaissance Orbiter Context Camera (MRO CTX) images as a base-map at 8192 pixels per degree to differentiate the geologic units from one another (Figure 2).

Discussion: The origin of the olivine is not immediately clear and is still under investigation, but may be related to several different formation mechanisms: (1) an ancient valley network infilled with olivine-enriched materials which has since been eroded resulting in inverted topography, (2) an ancient branching lava tube system or (3) another unknown geologic process. At the moment, most evidence supports this first formation mechanism (an ancient infilled valley network), due largely to the sinuosity of the feature and the evidence for extensive surface erosion throughout the region. This erosion likely removed any confining topographic valley and the central portion of the channel and, instead, resulted in the relative resistance of the high thermal inertia and olivine-rich marginal ridges. While not ruling out an eroded lava tube origin for this feature, it is unlikely because of its highly dendritic nature, which is uncommon in martian lava tubes [12]. Future work will focus on gathering additional morphological, spectral, and thermophysical information to further test these formation hypotheses.

Summary and Future Work: If this feature is in fact a valley network that has been infilled by an olivine-enriched basaltic material, buried and subsequently exhumed, it maybe be one of the oldest valley networks identified to date. The stratigraphic relationship of this feature is straightforward as other fluvial features clearly superpose this proposed valley network and are formed in the unit that would have fully buried this proposed valley network. While we are still determining the origin and processes which formed this feature, we have a clear idea of the structure from careful mapping of the main channel and surrounding olivine-rich rubble pile. While datasets over this site are somewhat limited, CTX derived digital terrain models will be created if suitable and CRISM compositional data (though primarily Mapping products exist) will be used to further strengthen the observation set. As more detailed analysis is carried out, we will continue to refine our hypotheses, maps, and incorporate new datasets.

Acknowledgements: This work was funded in part by the Mars Odyssey THEMIS project.

References: [1] P. G. Lucey (2004) *GRL, 31,* L08701. [2] V. E. Hamilton et al., (2005) *Geology, 33(6)*, 433-436. [3] M. J. Gaffey (2011) *AIP, 1386,* 129 [4] T. M. Hoefen et al., (2003) *Science, 302*, 627-630. [5] J. W. Head et al., (2003) *Nature, 426*, 797-802. [6] B. L. Ehlmann et al., (2014) *Annual Review of Earth and Planetary Sciences, 42,* 291-315. [7] J. L. Bandfield et al., (2013) *Icarus, 222(1),* 188-199. [8] E. Hamilton, M. M. Osterloo, and B. S. McGrane (2007) LPS XXXVIII, Abstract #1725. [9] J. Hil et al., (2014) *LPI #1791,* 1141. [10] C. S. Edwards, P. R. Christensen, and J. Hill (2011) *J. Geophys. Res., 116,* E10005. [11] K. J. Norwicki et al., (2013) *5th WHISPERS, 1-4.* [12] R. J. Leveille et al., (2010) *Planetary and Space Science, 58,* 592- 598.